Article

Feeling of Safety and Comfort Towards a Socially Assistive Unmanned Aerial Vehicle That Monitors People in a Virtual Home

Lidia M. Belmonte [1,2], Arturo S. García [2,3], Rafael Morales[1,2], José L. de la Vara [2,3], and Antonio Fernández-Caballero [2,3,4,*]

1 Departamento de Ingeniería Eléctrica, Electrónica, Automática y Comunicaciones, Universidad de Castilla-La Mancha, 02071-Albacete, Spain; rafael.morales@uclm.es
2 Universidad de Castilla-La Mancha, Instituto de Investigación en Informática de Albacete, 02071-Albacete, Spain
3 Departamento de Sistemas Informáticos, Universidad de Castilla-La Mancha, 02071-Albacete, Spain; antonio.fdez@uclm.es
4 CIBERSAM (Biomedical Research Networking Center in Mental Health), 28016-Madrid, Spain
* Correspondence: antonio.fdez@uclm.es; Tel.: +34 967599200 (A.F.-C.)

Abstract: Unmanned aerial vehicles (UAVs) represent a new model of social robots for home care of dependent persons. In this regard, this article introduces a study on people's feeling of safety and comfort while watching the monitoring trajectory of a quadrotor dedicated to determining their condition. Three main parameters are evaluated: the relative monitoring altitude, the monitoring velocity and the shape of the monitoring path around the person (ellipsoidal or circular). For this purpose, a new trajectory generator based on a state machine, which is successfully implemented and simulated in MATLAB/Simulink®, is described. The study is carried out with 37 participants using a virtual reality (VR) platform based on two modules, UAV Simulator and VR Visualiser, both communicating through the MQTT protocol. The participants' preferences have been a high relative monitoring altitude, a high monitoring velocity and a circular path. These choices are a starting point for the design of trustworthy socially assistive UAVs flying in real homes.

Keywords: Unmanned Aerial Vehicle (UAV); Social Robot; Feeling of Safety and Comfort; Trajectory Planning; Virtual Reality; MATLAB/Simulink®; MQTT

1. Introduction

Over the last decade, there has been an ever growing interest in human-robot interaction (HRI) not only in traditional industrial fields but also in emerging areas as homes [1]. Noteworthy, personal aerial robotics is becoming more and more pervasive to our home environments. Therefore, it seems vital to understand how home drones are perceived and understood by inhabitants to be fully accepted [2]. Within the broad class of personal robots, assistive robots for the elderly use to be grouped into rehabilitation and socially assistive robots [3]. The manner people accept social assistive robots in their life is still unknown [1]. Moreover, one-third of assistive technologies are abandoned within one year of use [4]. For this reason, the acceptability of social assistive robots is an essential aspect to overcome the resistance toward them. This is why, acceptance tests for assistive robots caring of elder adults are being highly demanded [3,4].

Social robot capabilities include approaching people in a natural manner [5] employing affective elements close to human-human interactions [6]. In this sense, the concept of trust is very important in the adoption of technologies to assist older adults at home [7,8]. Trust can be defined as an attitudinal judgement of the degree to which a user (the ageing adult) can rely on an agent (the social assistive robot) to achieve its goals under conditions of uncertainty [9]. People are more reluctant to engage with robots if negative consequences are more likely, and once confidence has been lost, people take

 doi:10.20944/preprints202010.0174.v1

longer to use this technology again [6,10]. Moreover, safety and efficiency of HRI collaboration often depend on appropriately calibrating trust towards the robot [9] and using a user-centred approach to realise what impacts the development of trust [11]. To date, trust regarding older adults' adoption of assistive technology has been determined in several ways, including whether the elderly feels safe and comfortable with the proposed solution [12–15]. The evaluation of these variables requires advanced physical prototyping or, as an alternative, virtual reality (VR) as a simulation tool allows for fast, flexible and iterative testing processes [16–18].

This paper deals with the use of unmanned aerial vehicles (UAVs) as socially assistive robots for dependent people, including ageing adults [19,20]. As it is essential to build a relationship of trust between the person and the flying assistive robot towards a full acceptance from the perspective of the assisted human. It is fundamental to consider the comfort and well-being of the end user. In this sense, the social UAV must carry out its mission, helping the person, but interrupting as little as possible his/her daily routine. The UAV should be seen as positive and not as a hindrance or even a danger to the person. More concretely, this paper introduces an assistive UAV for home care of dependent people. The mission of the robot is to perform a monitoring flight from time to time to determine his/her condition [21] and the possible assistance. This monitoring flight basically consists of a series of manoeuvres to take-off, get close to the person, fly around him/her to obtain facial images and then return to its base. This way, the main interaction between the socially assistive UAV and the person resides in the central part of the monitoring process, the flight around the assisted person.

In order to evaluate the users' sense of safety and comfort, a survey was conducted in which the participants evaluated different parameters of the UAV's trajectory during the monitoring process in a VR environment. The used VR platform consists of two modules interconnected by means of the Message Queuing Telemetry Transport (MQTT) protocol. The modules are (i) a complete UAV Simulator that includes the trajectory generator for the monitoring process, the control scheme and the dynamic model of a quadrotor, and, (ii) a VR Visualiser in which a quadrotor's 3D model performs the monitoring process of an avatar in a virtual home. By using this platform, each participant was able to experiment in first-person the UAV's monitoring process, i.e. a person was able to test different monitoring paths for the sake of commenting which one made him/her feel more comfortable as well as to evaluate other aspects regarding safety and privacy.

In the study, we focused on analysing three key parameters of the monitoring process; (i) the relative flight height, (ii) the speed of the UAV during the lap to the person, and finally, (iii) the shape of the trajectory that the UAV follows around him/her, considering two main options, namely, a circular path, which leads to maintain a constant distance between the person and the UAV, and an ellipsoidal one where the distance changes along the way. It should be noted that it was necessary to develop a new algorithm of trajectory planning for a quadrotor model, whose mathematical basis is explained in detail in this paper, to implement these options. This way, the article presents the results of a VR-based trust study considering feelings of safety and comfort on the trajectories followed by a socially assistive quadrotor while monitoring a person. The conclusions of this study will allow us to continue our challenging research project on assistive UAVs to advance in home care of dependent people.

The remainder of the article is structured as follows. Section 2 describes the main characteristics of the overall system including the virtual reality platform. Section 3.1 details the mathematical development of the new ellipsoidal trajectory planner implemented to carry out the study with the participants. Section 4 details the safety and comfort evaluation study regarding the monitoring parameters studied. Section 5 offers the results of the study. Finally, Section 6 summarises the conclusions of the work and introduces some future research lines.

2. General Description of the System

The proposed socially assistive robot's main mission is to serve as a tool for in-home monitoring of the dependent person in order to enable recording of images that can be analysed to determine his/her condition and the possible assistance that would be needed. This way, it is possible to provide the

Preprints (www.preprints.org) | NOT PEER-REVIEWED | Posted: 8 October 2020 doi:10.20944/preprints202010.0174.v1

patient with help or support and improve his/her quality of life. As mentioned above, the monitoring process basically consists in a flight around the person's position to obtain images of the face. During the flight around the person, a visual interaction between the robot and the assisted person is produced. The objective of this work is to analyse how this monitoring path should be in order to elicit the highest degree of safety and comfort feelings in the monitored person. For this reason, three key parameters, which are detailed below, are proposed.

The first parameter is the *relative monitoring altitude* (z_r), that is, the height with respect to the monitored person's head (z_p) at which the UAV performs the supervisory flight; i.e. the monitoring altitude will be given by expression $z_m = z_p + z_r$. As shown in Figure 1, the relative altitude parameter can be positive, negative, or even null, giving rise to three possible options in the monitoring process: (i) the UAV is located above the line of sight of the monitored person ($z_r > 0$), (ii) the aircraft is located in the line of sight ($z_r = 0$), and, (iii) the aircraft is located below the line of sight ($z_r < 0$).

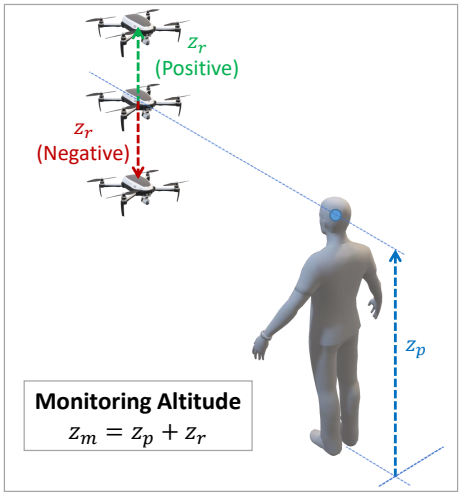

Figure 1. 3D representation in isometric perspective of the UAV's monitoring altitude, z_m, which is determined by the person's height, z_p, plus the *relative monitoring altitude*, z_r.

The second parameter is the *monitoring velocity* (ω_m), that is, the speed at which the UAV moves during the flight around the assisted person. This velocity will directly influence the monitoring time and is, therefore, a parameter whose value should be subject to positive validation by the users, since it can greatly influence the feelings of comfort and safety of the monitored person. In this case, the participants have been consulted regarding three possible options for the *monitoring velocity* as will be detailed later. Finally, the third parameter is the *monitoring radius*, i.e. the distance at which the UAV is placed from the person's position during the monitoring flight. This radius can be constant, which leads the UAV to trace a circular path around the person being monitored, or it can be variable, resulting in an elliptical path. For this reason, we also refer to this parameter as the monitoring trajectory (or the shape of the trajectory). Figure 2 shows the three possible options: (a) elliptical trajectory with the UAV close to the person's face, (b) circular trajectory with a constant distance between the UAV and the person, and (c) elliptical trajectory but with the UAV away from the person's face and closer to his/her side.

As can be inferred from the above parameters, the monitoring process is closely related to the position and orientation of the assisted person. Therefore, the trajectory planner needs to know these two variables at all time. Based on this information, the planner determines the reference signal for the position and yaw angle of the UAV for the different manoeuvres that make up the entire monitoring process. These references are the entry of the control algorithm that finally calculates the inputs to be applied for the UAV to perform the flight correctly.

Figure 3 represents the general scheme of the socially assistive UAV Simulator implemented in MATLAB/Simulink®. It shows the different blocks that compose it, which are: the dynamic model of

Preprints (www.preprints.org) | NOT PEER-REVIEWED | Posted: 8 October 2020 doi:10.20944/preprints202010.0174.v1

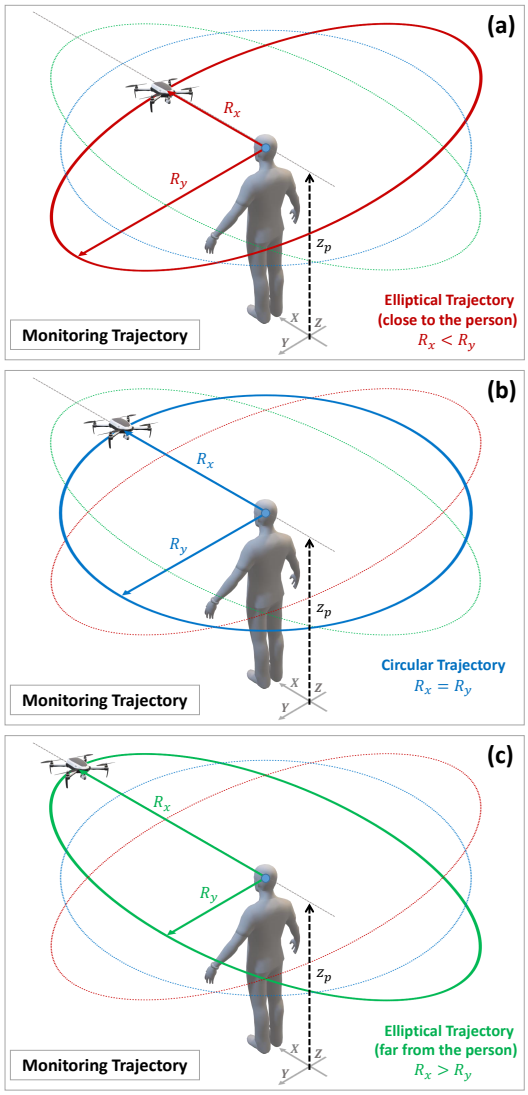

Figure 2. 3D representation in isometric perspective of the trajectory according to the UAV's *monitoring radius*: (a) elliptical trajectory close to the person's face ($R_x > R_y$); (b) circular trajectory in which the *monitoring radius* is constant ($R_x = R_y$); (c) elliptical trajectory far from the person's face ($R_x < R_y$).

a quadrotor UAV, the nonlinear control algorithm, and finally the trajectory planner for the monitoring process. At this respect, it should be mentioned that: (i) this UAV Simulator is part of a virtual reality platform developed by our research group, whose operation will be explained in Section 4; (ii) the dynamics of the quadrotor and the generalised proportional integral (GPI) controller can be consulted in a previous work [22]. Regarding the trajectory planner, the initial versions [16,23] were designed for a circular monitoring path at a constant height defined by the person's head. However, to carry out the study of the influence of the above-mentioned parameters in the safety and comfort of the monitored user, it has been necessary to implement a new trajectory planner algorithm which will be detailed next.

3. Trajectory Planning

This section describes the new ellipsoidal trajectory planning algorithm for the monitoring flight of a quadrotor UAV. It consists of a state machine in which the reference signals for the UAV's position and yaw angle are defined in each of the manoeuvres necessary to complete the monitoring process. It should be recalled that the signals generated by the path planner are the (reference) inputs of the UAV's

Preprints (www.preprints.org) | NOT PEER-REVIEWED | Posted: 8 October 2020 doi:10.20944/preprints202010.0174.v1

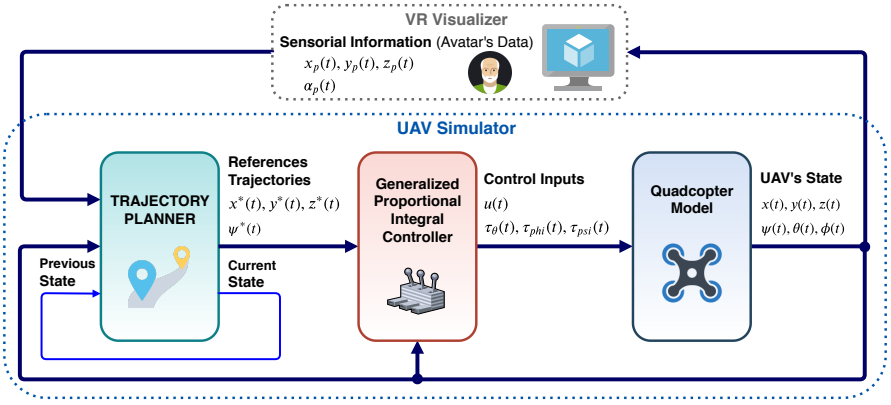

Figure 3. General diagram of the UAV Simulator which receives from the VR Visualiser the information concerning the person's avatar to calculate the reference trajectories used by the controller to guide the UAV in the monitoring process while returns the aircraft's position and orientation to represent its flight in a virtual home environment.

controller which in the end calculates what (control) inputs should be applied to the aircraft to direct its flight correctly during the monitoring of the person. In this process, the information captured by the camera on board the UAV will be sent to a processing station for analysis using artificial intelligence techniques, such as emotion recognition, to determine the person's condition and possible assistance.

Before detailing the equations of the different states that make up the planner, we proceed to define the mathematical basis for plotting the ellipsoidal path around the person (an ellipse on the horizontal plane defined by the monitoring height, centred on the person's position and rotated according to his/her direction).

3.1. Equations of the Ellipse

Firstly, the main path of the monitoring process consists in an ellipse in the horizontal plane (XY) whose mathematical equation in the simplest case (centred at the origin) is the following:

$$\frac{x^2}{R_x^2} + \frac{y^2}{R_y^2} = 1 \tag{1}$$

where R_x is the radius on the X axis and R_y is the radius on the Y axis.

However, we must consider that the ellipse will be centred on the position of the person, therefore its equation would be as follows:

$$\frac{(x - C_x)^2}{R_x^2} + \frac{(y - C_y)^2}{R_y^2} = 1 \tag{2}$$

where R_x and R_y are the radius on the X and Y axes, respectively, and (C_x, C_y) are the coordinates of the centre of the ellipse that will coincide with the person's horizontal position, (x_p, y_p).

Moreover, we must consider that the ellipse will also be rotated an angle of θ rad, according to the orientation of the person (α_p), and therefore the equation will be expressed as follows:

$$\frac{((x - C_x) \cdot \cos(\theta) + (y - C_y) \cdot \sin(\theta))^2}{R_x^2} + \frac{((x - C_x) \cdot \sin(\theta) - (y - C_y) \cdot \cos(\theta))^2}{R_y^2} = 1 \tag{3}$$

where R_x and R_y are the radius on the X and Y axes, respectively, (C_x, C_y) are the coordinates of the centre of the ellipse, and θ is the above-mentioned rotation angle.

Preprints (www.preprints.org) | NOT PEER-REVIEWED | Posted: 8 October 2020 doi:10.20944/preprints202010.0174.v1

To conclude, Eq. (4) details the parametric formula depending on the variable γ of an ellipse centred at the position (C_x, C_y), and rotated at a certain angle θ. Figure 4 represents this parameterisation in the particular case of the monitoring process, i.e. when the ellipse is centred and rotated according to the person's position and orientation, respectively $((C_x, C_y) = (x_p, y_p); \theta = \alpha_p)$. This parametric equation will be useful for the generation of the reference path for the UAV's XY position as will be explained bellow.

$$\begin{aligned} x(\gamma) &= C_x + R_x \cos(\gamma)\cos(\theta) - R_y \sin(\gamma)\sin(\theta) \\ y(\gamma) &= C_y + R_x \cos(\gamma)\sin(\theta) + R_y \sin(\gamma)\cos(\theta) \end{aligned} \tag{4}$$

where:

- C_x is the X-coordinate of the centre [m]
- C_y is the Y-coordinate of the centre [m]
- R_x is the radius on the X-axis [m]
- R_y is the radius on the Y-axis [m]
- θ is the rotation angle [rad]
- γ is the parameter, which ranges from 0 to 2π [rad]

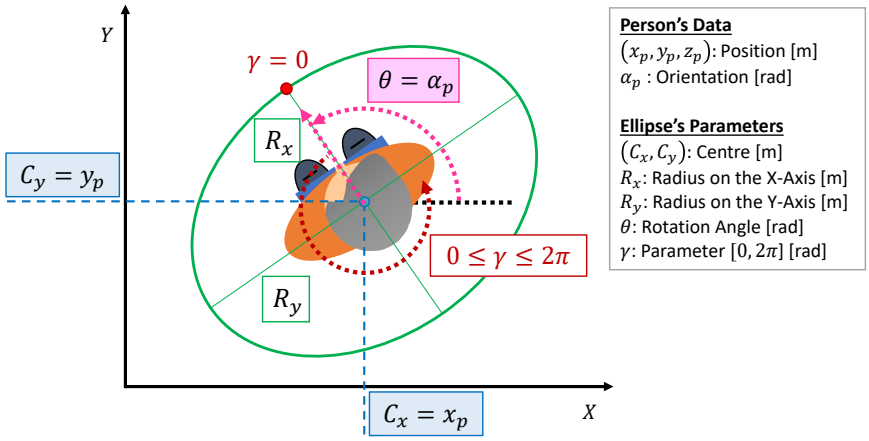

Figure 4. Variables of the parametric equation of the ellipse centred at the XY position of the person and rotated according to his/her orientation.

3.2. Determination of the Safety Position

The safety position is the point at which the UAV approaches after take-off (to approximate the patient's immediate surroundings) and from which it begins to rotate around the person to take images that will be sent for analysis. After completing the data capture lap, the UAV returns from this safety position to the base position for landing. Therefore, the safety position is an important way-point in the monitoring process whose calculation is explained next. In the case of considering an ellipsoidal monitoring trajectory, the XY coordinates of the safety position will be determined by the nearest intersection between the imaginary line connecting the centre of the person and the position of the UAV with the ellipse centred and rotated according to the person's position and orientation (see Figure 5). It should be recalled that the Z coordinate of this safety position will be given by the UAV's altitude in the monitoring process (person's head height plus relative altitude parameter).

This way, the problem raised is: (1) determine the points of intersection of a line passing through the centre of the ellipse and the position of the UAV with the ellipse rotated and centred on the person; (2) determine the point of intersection closest to the position of the UAV. The mathematical resolution is detailed below.

Preprints (www.preprints.org) | NOT PEER-REVIEWED | Posted: 8 October 2020 doi:10.20944/preprints202010.0174.v1

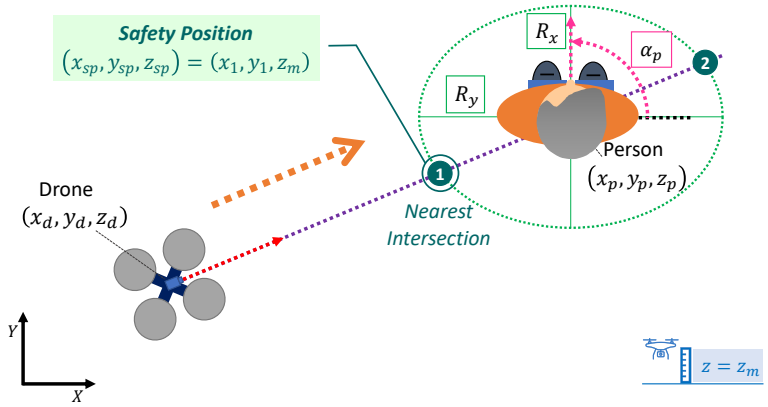

Figure 5. Determination of the safety position (x_{sp}, y_{sp}, z_{sp}) to which the UAV is approaching to start the elliptical monitoring lap around the person.

3.2.1. Calculation of the Intersection Points with the Rotated Ellipse

The equation of a line defined by two points, (x_a, y_a) and (x_b, y_b) is detailed in Eq. (5).

$$y = y_a + \frac{y_b - y_a}{x_b - x_a} \cdot (x - x_a); \tag{5}$$

The above can also be expressed in parametric form, thus giving rise to two individual expressions for each component of the horizontal plane (XY) dependent on the t parameter:

$$\begin{aligned} x(t) &= x_a + (x_b - x_a) \cdot t; \\ y(t) &= y_a + (y_b - y_a) \cdot t; \end{aligned} \tag{6}$$

If the point (x_a, y_a) matches with the centre of the ellipse around the person (x_p, y_p), and the point (x_b, y_b) is the UAV's position, (x_d, y_d), the parametric Eq. (6) can be written as follows:

$$\begin{aligned} x(t) &= x_p + (x_d - x_p) \cdot t; \\ y(t) &= y_p + (y_d - y_p) \cdot t; \end{aligned} \tag{7}$$

In order to calculate the intersection between the line defined by Eq. (6) and the ellipse defined by the person's pose, i.e. centred and rotated according to his/her position and orientation, $(C_x, C_y) = (x_p, y_p); \theta = \alpha_p$, it is necessary to substitute Eq. (7) in Eq. (3), obtaining:

$$\begin{aligned} &\frac{((x_p + (x_d - x_p) \cdot t - x_p) \cdot \cos(\alpha_p) + (y_p + (y_d - y_p) \cdot t - y_p) \cdot \sin(\alpha_p))^2}{R_x^2} + \\ &\frac{((x_p + (x_d - x_p) \cdot t - x_p) \cdot \sin(\alpha_p) - (y_p + (y_d - y_p) \cdot t - y_p) \cdot \cos(\alpha_p))^2}{R_y^2} = 1 \end{aligned} \tag{8}$$

$$\begin{aligned} &\frac{(((x_d - x_p) \cdot t) \cdot \cos(\alpha_p) + ((y_d - y_p) \cdot t) \cdot \sin(\alpha_p))^2}{R_x^2} + \\ &\frac{(((x_d - x_p) \cdot t) \cdot \sin(\alpha_p) - ((y_d - y_p) \cdot t) \cdot \cos(\alpha_p))^2}{R_y^2} = 1 \end{aligned} \tag{9}$$

After some operations, Eq. (9) is simplified and the result is detailed in Eq. (10):

$$\frac{t^2 \cdot f_1}{R_x^2} + \frac{t^2 \cdot f_2}{R_y^2} = 1 \tag{10}$$

Preprints (www.preprints.org) | NOT PEER-REVIEWED | Posted: 8 October 2020 doi:10.20944/preprints202010.0174.v1

where

$$\begin{aligned} f_1 &= (x_d^2 + x_p^2 - 2x_d x_p) \cdot \cos^2(\alpha_p) + (y_d^2 + y_p^2 - 2y_d y_p) \cdot \sin^2(\alpha_p) + \\ &\quad 2 \cdot (x_d - x_p) \cdot (y_d - y_p) \cdot \cos(\alpha_p) \cdot \sin(\alpha_p); \\ f_2 &= (x_d^2 + x_p^2 - 2x_d x_p) \cdot \sin^2(\alpha_p) + (y_d^2 + y_p^2 - 2y_d y_p) \cdot \cos^2(\alpha_p) - \\ &\quad 2 \cdot (x_d - x_p) \cdot (y_d - y_p) \cdot \sin(\alpha_p) \cdot \cos(\alpha_p); \end{aligned}$$

Now, from Eq. (10) it is possible to obtain the expression of the parameter t, and from that determine two possible solutions, t_1 and t_2, using Eq. (12) and Eq. (13), respectively:

$$t = \frac{R_x \cdot R_y}{\sqrt{f_1 \cdot R_y^2 + f_2 \cdot R_x^2}} \tag{11}$$

- Solution 1:

$$t_1 = \frac{R_x \cdot R_y}{\sqrt{f_1 \cdot R_y^2 + f_2 \cdot R_x^2}} \tag{12}$$

- Solution 2:

$$t_2 = -t_1 = -\frac{R_x \cdot R_y}{\sqrt{f_1 \cdot R_y^2 + f_2 \cdot R_x^2}} \tag{13}$$

Substituting the two solutions of the t parameter, t_1 and t_2, in the parametric Eq. (7), we obtain the two points of intersection between the rotated ellipse and the line joining the position of the UAV with the centre of the ellipse (the position of the person):

- Solution 1:

$$\begin{aligned} x_1 = x(t_1) &= x_p + (x_d - x_p) \cdot t_1; \\ y_1 = y(t_1) &= y_p + (y_d - y_p) \cdot t_1; \end{aligned} \tag{14}$$

- Solution 2:

$$\begin{aligned} x_2 = x(t_2) &= x_p + (x_d - x_p) \cdot t_2; \\ y_2 = y(t_2) &= y_p + (y_d - y_p) \cdot t_2; \end{aligned} \tag{15}$$

3.2.2. Determination of the Nearest Intersection Point (Safety Position)

Finally, to determine the safety position (x_{sp}, y_{sp}), it is necessary to know which intersection point is closest to the position of the UAV (see example in Figure 5). To do this, we calculate the distance between the UAV and the two candidates calculated above:

$$\begin{aligned} d_1 &= \sqrt{(x_1 - x_d)^2 + (y_1 - y_d)^2}; \\ d_2 &= \sqrt{(x_2 - x_d)^2 + (y_2 - y_d)^2}; \end{aligned} \tag{16}$$

Thus, if the distance d_1 is equal to or less than d_2, the first point will be the safety position in the monitoring process, $(x_{sp}, y_{sp}) = (x_1, y_1)$. Conversely, if the distance d_2 is less than d_1, the safety position will be the second point, $(x_{sp}, y_{sp}) = (x_2, y_2)$. Please remember that the Z coordinate of this safety position will be given by the altitude of the UAV in the monitoring process, z_m (person's height plus relative height parameter).

Preprints (www.preprints.org) | NOT PEER-REVIEWED | Posted: 8 October 2020 doi:10.20944/preprints202010.0174.v1

3.3. Ellipsoidal Trajectory around the Person

To generate the reference ellipsoidal path around the person, it is necessary to convert the safety position at which the UAV stops for a time before turning around him or her into the corresponding value of the parameter γ of the parametric equation of the ellipse, Eq. (4). To do this, we first calculate the position in the original ellipse (x_{e_o}, y_{e_o}), an ellipse without rotation and centred at the point $(0,0)$, to which corresponds the safety position in the rotated and person-centred ellipse, $PosE_{Rot} = (x_{sp}, y_{sp})$. In this way, and using matrix notation, we obtain:

$$\underbrace{\begin{bmatrix} x_{sp} \\ y_{sp} \end{bmatrix}}_{PosE_{Rot}} = \underbrace{\begin{bmatrix} cos(\alpha_p) & -sin(\alpha_p) \\ sin(\alpha_p) & \cos(\alpha_p) \end{bmatrix}}_{MAT_{ROT}} \cdot \underbrace{\begin{bmatrix} x_{e_o} \\ y_{e_o} \end{bmatrix}}_{PosE_{Orig}} + \underbrace{\begin{bmatrix} x_p \\ y_p \end{bmatrix}}_{Centre} \tag{17}$$

$$\begin{bmatrix} x_{e_o} \\ y_{e_o} \end{bmatrix} = \begin{bmatrix} cos(\alpha_p) & -sin(\alpha_p) \\ sin(\alpha_p) & \cos(\alpha_p) \end{bmatrix}^{-1} \cdot \begin{bmatrix} x_{sp} - x_p \\ y_{sp} - y_p \end{bmatrix} \tag{18}$$

Secondly, and depending on the quadrant in which the calculated position is located in the original ellipse, (x_{e_o}, y_{e_o}), the value of the parameter γ is determined using the inverse of the cosine or sine functions as follows:

- Quadrant I: $x_{e_o} > 0, \quad y_{e_o} > 0$

$$\gamma = \arccos\left(\frac{x_{e_o}}{R_x}\right) = \arcsin\left(\frac{y_{e_o}}{R_y}\right) \tag{19}$$

- Quadrant II: $x_{e_o} < 0, \quad y_{e_o} > 0$

$$\gamma = \arccos\left(\frac{x_{e_o}}{R_x}\right) = \pi - \arcsin\left(\frac{y_{e_o}}{R_y}\right) \tag{20}$$

- Quadrant III: $x_{e_o} < 0, \quad y_{e_o} < 0$

$$\gamma = 2\pi - \arccos\left(\frac{x_{e_o}}{R_x}\right) = \pi - \arcsin\left(\frac{y_{e_o}}{R_y}\right) \tag{21}$$

- Quadrant IV: $x_{e_o} > 0, \quad y_{e_o} < 0$

$$\gamma = 2\pi - \arccos\left(\frac{x_{e_o}}{R_x}\right) = 2\pi + \arcsin\left(\frac{y_{e_o}}{R_y}\right) \tag{22}$$

Once we know the value of the γ parameter to which corresponds the initial position from which the ellipsoidal path around the person will start, that is, the equivalent to the safety position ($\gamma_{initial} = \gamma_{sp}$), we can use the parametric formula of the ellipse, Eq. (4), and gradually increase its parameter to complete one lap ($\gamma_{initial} + 2\pi$ rad). This will be the procedure used to obtain the reference trajectories for the UAV's XY position for the ellipse around the person as detailed below.

3.4. States of the Trajectory Planner

This section describes in the detail the states that compose the new trajectory planner for the monitoring process considering an ellipsoidal path around the monitored person. In the previous version of the planner [16], the path around the person was circular. It is worth mentioning that this particular case can also be implemented using the equations described below simply by taking $R_x = R_y$. Compared to the previous version, in which the monitoring flight was only performed at a constant height defined by the person's head, it is now also possible to vary this height by the above-mentioned parameter of *relative monitoring altitude* (z_r). In this way, the UAV in the monitoring

Preprints (www.preprints.org) | NOT PEER-REVIEWED | Posted: 8 October 2020 doi:10.20944/preprints202010.0174.v1

process will fly at the same height as the person (coinciding with his/her line of sight), at a higher height than this (above the line of sight), or at a lower height (below the line of sight).

Before describing the states of the planner, it should be mentioned the following assumptions have been considered in its development: (i) the UAV remains in its base position before and after a monitoring process (x_b, y_b, z_b); (ii) the information of the monitored person's position, (x_p, y_p, z_p), and orientation, α_p, are known at each moment; (iii) the reference trajectories are defined so that the UAV's camera always points in its forward direction or towards the person; (iv) there are no energy limitations since the monitoring process is carried out in a short period of time; and, (v) consequently, it is presumed that the person does not walk during this brief process. The states of the trajectory planner are a total of twelve represented graphically in Figure 6 and whose equations for the position and orientation of the UAV are summarised in Table 1 and Table 2. The details of each state are as follows.

- STATE 0 - Home: Represents the UAV waiting in its base position, (x_b, y_b, z_b), and initially oriented with a yaw angle, $\psi(0)$, which by default is equal to 0 rad. When it receives the instruction to start the monitoring process, it transits to state 1.
- STATE 1 - Takeoff: This is the first manoeuvre to raise the UAV, with a constant speed v_z, from the base level, z_b, until the monitoring altitude, z_m. This level will be equal to the person's height (measured in the centre of his/her head, z_p) plus the relative altitude parameter (z_r), which can be positive, zero, or even negative to consider the three scenarios mentioned before (above his/her line of sight, coinciding with it or below it). Thus, when the UAV reaches the monitoring level, $z_m = z_p + z_r$, the planner switches to state 2.
- STATE 2 - Person Search: After takeoff, the UAV is requested to turn, varying the yaw angle with a speed defined by ω_ψ, in order to find the person with its on board camera. Since the person's position is known at each moment, it is possible to calculate the final (target) yaw angle, ψ_{f2}, which will be the difference between the angle $\alpha = arctan(\frac{y_p - y_{i2}}{x_p - x_{i2}})$ and the camera's angle α_{camera} as can be observed in Figure 6(a). Therefore, the yaw angle is gradually modified until the UAV's camera is focused on the person. At this moment, the planner transits to state 3.
- STATE 3 - Approximation: The UAV must approach the person (already centred on the camera's view) to turn around him/her in the next states. As detailed in Subsection 3.2, the UAV must reach the safety position whose XY coordinates will be given by the nearest intersection of the (imaginary) line joining the positions of the UAV and the person with the ellipse centred and rotated according to his/her position and direction, respectively. The *relative monitoring altitude* should be maintained constant, i.e., the Z coordinate of the safety position will match with the monitoring level. The planner will transit to state 4 once the UAV reaches the safety position (x_{sp}, y_{sp}, z_{sp}).
- STATE 4 - Waiting in Safety Position: Intermediate state in which the UAV waits for a short time to start later the lap around the person more precisely. Therefore, once the programmed time (t_{s4}) has elapsed, it transits to state 5.
- STATE 5 - Face Search: At this moment, the ellipsoidal rotation of the UAV around the person starts from the safety position (whose equivalence to the parameter γ of the ellipse's parametric formula is determined according to Eq. (17)-(22)), while the flight height is keeping constant. On the other hand, the UAV's yaw angle is modified during the ellipsoidal trajectory so that its on board camera is always pointing towards the person. This way, once the UAV's camera finds the person's face, the planner switches to state 6. It should be noted at this point that, since the person's information is known at all times, and the ellipse is rotated according to his/her direction, $\theta = \alpha_p$, the position in front of his/her face, labelled as photo position in Figure 6(d), (x_{ph}, y_{ph}, z_{ph}), can be calculated from the ellipse's parametrisation by taking $\gamma = 0$ [rad].
- STATE 6 - Data Capture: In the general case, the UAV can remain in the position in front of the person's face, (x_{ph}, y_{ph}, z_{ph}), to capture images with better accuracy. Once the data capture timer (t_{s6}) elapses, the planner transitions to state 7. On the contrary, if the UAV is programmed to

Preprints (www.preprints.org) | NOT PEER-REVIEWED | Posted: 8 October 2020 doi:10.20944/preprints202010.0174.v1

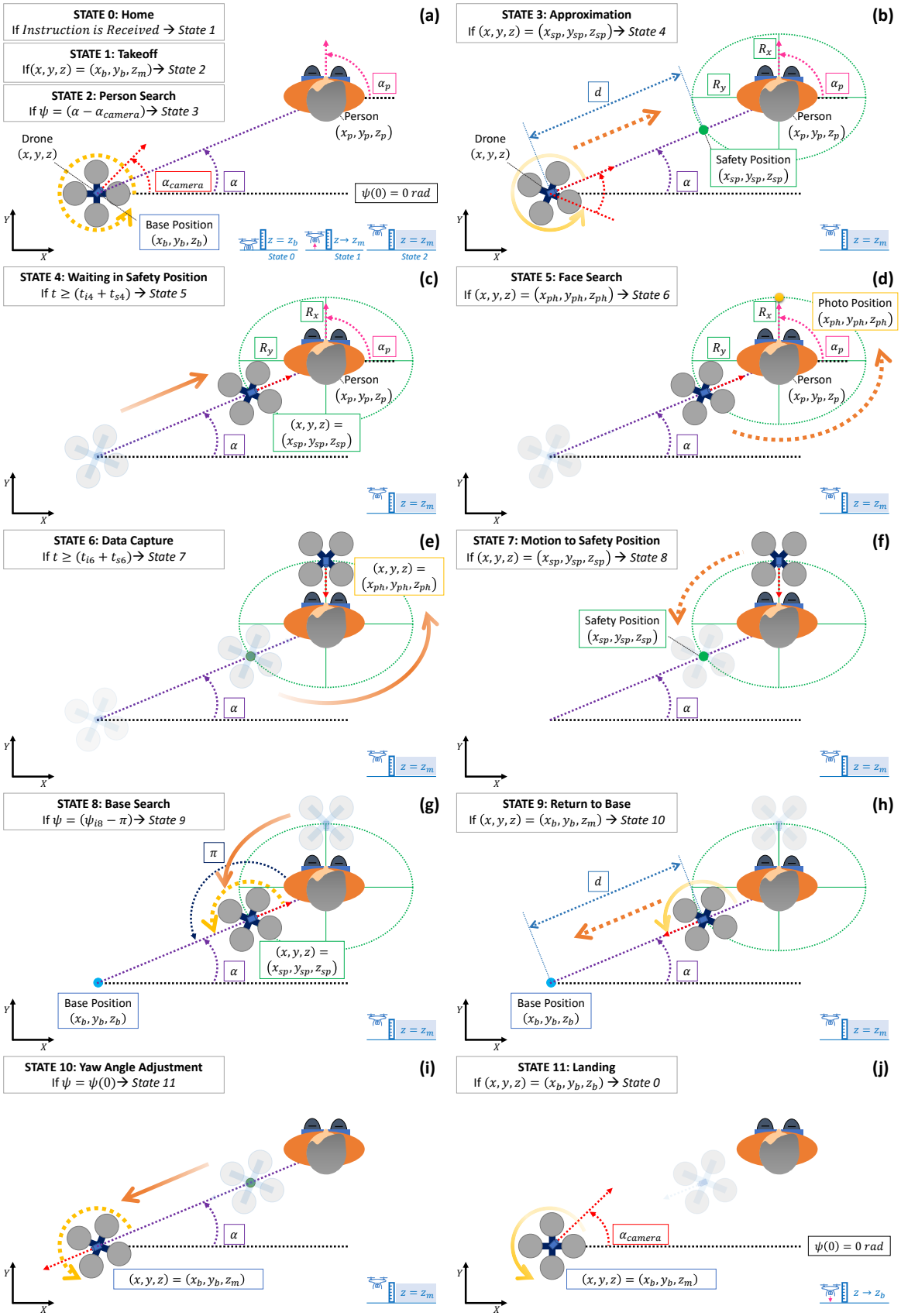

Figure 6. Graphical representation of the trajectory planner's states.

 doi:10.20944/preprints202010.0174.v1

take pictures of the person for the entire lap around him or her, the waiting time can be set to zero ($t_{s6} = 0$) and the planner would transit directly to state 7. The UAV would continue the lap without stopping.

- STATE 7 - Motion and Safety Position: The UAV will continue its ellipsoidal rotation around the monitored person to reach the safety position again. The height of the UAV will be kept constant and the yaw angle will be varied so that the on board camera continues to be pointed at the patient. Mathematically, it is, therefore, equal to state 5 and, consequently, the reference trajectories are determined in a very similar way. Once the UAV reaches the safety position, (x_{sp}, y_{sp}, z_{sp}), the planner transits to state 8.
- STATE 8 - Base Search: Once the UAV has completed its ellipsoidal trajectory around the monitored person, it is commanded to turn on itself, gradually adjusting its yaw angle to search for the base with its camera. In this way, a procedure similar to state 2 will be followed, but the final yaw angle is now known in advance. As can be seen in Figure 6(g)), the UAV must turn $-\pi$ rad, so that the UAV's camera directly points towards the base. At this point, the planner will switch to state 9.
- STATE 9 - Return to Base: The aircraft is ordered to return to over the base position while keeping the flight height constant. In this way, the UAV's movement is the same as state 3, but in the opposite direction, thus the reference trajectories are calculated in a similar way (in this case even the final position is known, so no additional calculation is necessary unlike state 3 in which the safety position was determined). Once the UAV is positioned over its base, at (x_b, y_b, z_m), the planner transits to state 10.
- STATE 10 - Yaw Angle Adjustment: Before landing, the yaw angle of the UAV is adjusted to its initial value to prepare the aircraft for future monitoring processes, while the UAV's position is keeping constant. The reference trajectories will be, therefore, analogous to state 2. This way, when the adjustment is completed, the planner will shift to state 11.
- STATE 11 - Landing: Finally the UAV is commanded to land at its base (x_b, y_b, z_b). In this way, the aircraft will descend vertically, with a constant speed defined by the parameter v_z, until reaching the base level, and the planner will transit to the initial state (0) to be ready for the next monitoring process.

Preprints (www.preprints.org) | NOT PEER-REVIEWED | Posted: 8 October 2020 doi:10.20944/preprints202010.0174.v1

Table 1. Trajectory planner's states for the monitoring process. (Part I - States from 0 to 7). Reference trajectories for the position (x, y, z) and yaw angle (ψ) of a quadrotor UAV monitoring a person whose position (x_p, y_p, z_p) and orientation $(\alpha_p)$are known.

State	Reference Trajectories	Parameters and Condition [C]
0	$x_0^*(t) = x_b$ $y_0^*(t) = y_b$ $z_0^*(t) = z_b$ $\psi_0^*(t) = \psi(0)$	(x_b, y_b, z_b): base position [m] $\psi(0)$: initial yaw angle (by default 0) [rad] [C] If *Instruction is Received*→ State 1
1	$x_1^*(t) = x_{i1}$ $y_1^*(t) = y_{i1}$ $z_1^*(t) = z_{i1} + \left(\frac{t-t_{i1}}{t_{f1}-t_{i1}}\right) \cdot (z_m - z_{i1})$ $\psi_1^*(t) = \psi_{i1}$ where: $t_{f1} = t_{i1} + \left\lvert\frac{z_m - z_{i1}}{v_z}\right\rvert$; $z_m = z_p + z_r$	z_r: relative monitoring altitude [m] v_z: velocity in Z-Axis [m/s] [C] If $(x, y, z) = (x_b, y_b, z_m) \rightarrow$ State 2
2	$x_2^*(t) = x_{i2}$ $y_2^*(t) = y_{i2}$ $z_2^*(t) = z_{i2}$ $\psi_2^*(t) = \psi_{i2} + \left(\frac{t-t_{i2}}{t_{f2}-t_{i2}}\right) \cdot (\psi_{f2} - \psi_{i2})$ where: $t_{f2} = t_{i2} + \left\lvert\frac{\psi_{f2} - \psi_{i2}}{\omega_\psi}\right\rvert$; $\psi_{f2} = (\alpha - \alpha_{camera})$; $\alpha = arctan\left(\frac{y_p - y_{i2}}{x_p - x_{i2}}\right)$	ω_ψ: angular velocity (yaw) [rad/s] α_{camera}: camera's angle [rad] [C] If $\psi = \psi_{f2} = (\alpha - \alpha_{camera}) \rightarrow$ State 3
3	$x_3^*(t) = x_{i3} + v_d \cdot \frac{(x_{sp} - x_{i3})}{d} \cdot (t - t_{i3})$ $y_3^*(t) = y_{i3} + v_d \cdot \frac{(y_{sp} - y_{i3})}{d} \cdot (t - t_{i3})$ $z_3^*(t) = z_{i3}$ $\psi_3^*(t) = \psi_{i3}$ where: $d = \sqrt{(x_{sp} - x_{i3})^2 + (y_{sp} - y_{i3})^2}$; $(x_{sp}, y_{sp}) \Rightarrow$ see subsection 3.2	R_x: radius on the X-axis [m] R_y: radius on the Y-axis [m] v_d: diagonal velocity [m/s] [C] If $(x, y, z) = (x_{sp}, y_{sp}, z_{sp}) \rightarrow$ State 4
4	$x_4^*(t) = x_{i4}$ $y_4^*(t) = y_{i4}$ $z_4^*(t) = z_{i4}$ $\psi_4^*(t) = \psi_{i4}$	t_{s4}: timer [s] [C] If $t_{i4} + t_{s4} \rightarrow$ State 5
5	$x_5^*(t) = x_p + R_x \cos(\gamma)\cos(\alpha_p) - R_y \sin(\gamma)\sin(\alpha_p)$ $y_5^*(t) = y_p + R_x \cos(\gamma)\sin(\alpha_p) + R_y \sin(\gamma)\cos(\alpha_p)$ $z_5^*(t) = z_{i5}$ $\psi_5^*(t) = arctan\left(\frac{y_p - y_5^*(t)}{x_p - x_5^*(t)}\right) - \alpha_{camera}$ where: $\gamma = \gamma_{sp} + \omega_m \cdot (t - t_{i5})$; $\gamma_{sp} \Rightarrow$ see subsection 3.3 $\omega_m \Rightarrow$ see Table 3	R_x: radius on the X-axis [m] R_y: radius on the Y-axis [m] ω_m: monitoring angular velocity [rad/s] α_{camera}: camera's angle [rad] [C] If $(x, y, z) = (x_{ph}, y_{ph}, z_{ph}) \rightarrow$ State 6
6	$x_6^*(t) = x_{i6}$ $y_6^*(t) = y_{i6}$ $z_6^*(t) = z_{i6}$ $\psi_6^*(t) = \psi_{i6}$	t_{s6}: timer [s] [C] If $t_{i6} + t_{s6} \rightarrow$ State 7
7	$x_7^*(t) = x_p + R_x \cos(\gamma)\cos(\alpha_p) - R_y \sin(\gamma)\sin(\alpha_p)$ $y_7^*(t) = y_p + R_x \cos(\gamma)\sin(\alpha_p) + R_y \sin(\gamma)\cos(\alpha_p)$ $z_7^*(t) = z_{i7}$ $\psi_7^*(t) = arctan\left(\frac{y_p - y_7^*(t)}{x_p - x_7^*(t)}\right) - \alpha_{camera}$ where: $\gamma = \gamma_{ph} + \omega_m \cdot (t - t_{i7})$; $\gamma_{ph} = 0$ $\omega_m \Rightarrow$ see Table 3	R_x: radius on the X-axis [m] R_y: radius on the Y-axis [m] ω_m: monitoring angular velocity [rad/s] α_{camera}: camera's angle [rad] [C] If $(x, y, z) = (x_{sp}, y_{sp}, z_{sp}) \rightarrow$ State 8

Notation $\Rightarrow$ t_{in}: initial time of state n; t_{fn}: final time of state n; $x_{in} = x(t_{in})$: initial value of x coordinate at the beginning of state n (at instant t_{in}); $y_{in} = y(t_{in})$: initial value of y coordinate at the beginning of state y (at instant t_{in}); $z_{in} = z(t_{in})$: initial value of z coordinate at the beginning of state n (at instant t_{in}); $\psi_{in} = \psi(t_{in})$: initial value of ψ angle at the beginning of state n (at instant t_{in})

Preprints (www.preprints.org) | NOT PEER-REVIEWED | Posted: 8 October 2020 doi:10.20944/preprints202010.0174.v1

Table 2. Trajectory planner's states for the monitoring process. (Part II - States from 8 to 11). Reference trajectories for the position (x, y, z) and yaw angle (ψ) of a quadrotor UAV monitoring a person whose position (x_p, y_p, z_p) and orientation $(\alpha_p)$are known.

State	Reference Trajectories	Parameters and Condition [C]
8	$x_8^*(t) = x_{i8}$ $y_8^*(t) = y_{i8}$ $z_8^*(t) = z_{i8}$ $\psi_8^*(t) = \psi_{i8} + \left(\frac{t-t_{i8}}{t_{f8}-t_{i8}}\right) \cdot (\psi_{f8} - \psi_{i8})$ where: $t_{f8} = t_{i8} + \left\lvert \frac{\psi_{f8}-\psi_{i8}}{\omega_\psi} \right\rvert$; $\psi_{f8} = (\psi_{i8} - \pi)$	ω_ψ: angular velocity (yaw) [rad/s] [C] If $\psi = \psi_{f8} = (\psi_{i8} - \pi) \rightarrow$ State 9
9	$x_9^*(t) = x_{i9} + v_d \cdot \frac{(x_b - x_{i9})}{d} \cdot (t - t_{i9})$ $y_9^*(t) = y_{i9} + v_d \cdot \frac{(y_b - y_{i9})}{d} \cdot (t - t_{i9})$ $z_9^*(t) = z_{i9}$ $\psi_9^*(t) = \psi_{i9}$ where: $d = \sqrt{(x_b - x_{i9})^2 + (y_b - y_{i9})^2}$	(x_b, y_b, z_b): base position [m] v_d: diagonal velocity [m/s] [C] If $(x, y, z) = (x_b, y_b, z_m) \rightarrow$ State 10
10	$x_{10}^*(t) = x_{i10}$ $y_{10}^*(t) = y_{i10}$ $z_{10}^*(t) = z_{i10}$ $\psi_{10}^*(t) = \psi_{i10} + \left(\frac{t-t_{i10}}{t_{f10}-t_{i10}}\right) \cdot (\psi(0) - \psi_{i10})$ where: $t_{f10} = t_{i10} + \left\lvert \frac{\psi(0)-\psi_{i10}}{\omega_\psi} \right\rvert$	ω_ψ: angular velocity (yaw) [rad/s] ψ_0: initial yaw angle (by default 0) [rad] [C] If $\psi = \psi(0) \rightarrow$ State 11
11	$x_{11}^*(t) = x_{i11}$ $y_{11}^*(t) = y_{i11}$ $z_{11}^*(t) = z_{i11} + \left(\frac{t-t_{i11}}{t_{f11}-t_{i11}}\right) \cdot (z_b - z_{i11})$ $\psi_{11}^*(t) = \psi_{i11}$ where: $t_{f11} = t_{i11} + \left\lvert \frac{z_b - z_{i11}}{v_z} \right\rvert$	(x_b, y_b, z_b): base position [m] v_z: velocity in Z-Axis [m/s] [C] If $(x, y, z) = (x_b, y_b, z_b) \rightarrow$ State 0

Notation $\Rightarrow$ t_{in}: initial time of state n; t_{fn}: final time of state n; $x_{in} = x(t_{in})$: initial value of x coordinate at the beginning of state n (at instant t_{in}); $y_{in} = y(t_{in})$: initial value of y coordinate at the beginning of state y (at instant t_{in}); $z_{in} = z(t_{in})$: initial value of z coordinate at the beginning of state n (at instant t_{in}); $\psi_{in} = \psi(t_{in})$: initial value of ψ angle at the beginning of state n (at instant t_{in})

3.5. Simulation Results

The simulation results of the proposed ellipsoidal trajectory planner are presented now. The tests carried out in the UAV Simulator (in MATLAB/Simulink®) of the VR platform served also to generate the set of videos used in the questionnaire with the participants (which will be detailed in the following section). In this sense, the objective was to record 9 videos (three for each parameter). For that, three different values were considered for each parameter under study as detailed in Table 3. This would lead to testing 9 cases, however, the number of simulations carried out was only 7 because the two remaining parameters in each case were set at their intermediate value (the regular case coincides in the three parameters). In this way, multiple combinations were not considered because they might result in an excessive number of trials for the participants, which might lead to threats such as fatigue effect. Furthermore, the questionnaire is divided into three parts, according to the three parameters under study (*relative monitoring altitude*, *monitoring velocity*, and *monitoring radius*), and it is important that the participant concentrates on only one parameter (without considering the influence of the others).

The results of the simulation tests carried out using the settings shown in Table 4 are summarised in Figure 7. Each subfigure (a-g) corresponding to each test performed, represents in 3D the reference path generated by the planner (in blue) and the actual trajectory performed by the UAV (in red) during the monitoring process of a person whose head position and orientation (in pink) are known. It must

Preprints (www.preprints.org) | NOT PEER-REVIEWED | Posted: 8 October 2020 doi:10.20944/preprints202010.0174.v1

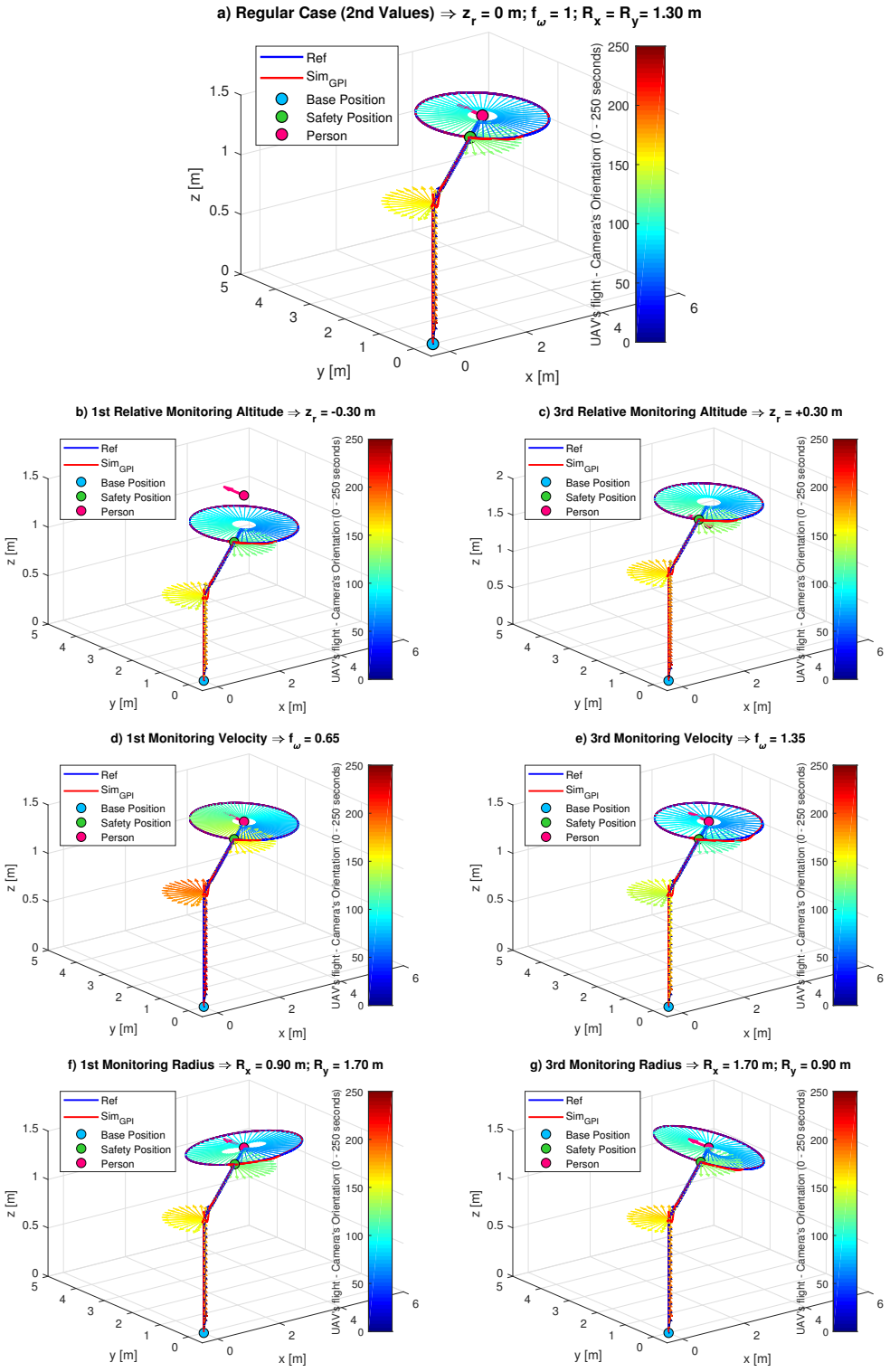

Figure 7. Results of the tests to verify the new ellipsoidal trajectory planner carried out using the UAV Simulator (part of the VR platform and implemented in MATLAB/Simulink®). For each test, the following is represented: (1) trajectory generated by the planner (in blue) against the actual trajectory performed by the quadrotor model as the result of the action of the GPI controller (in red); (2) orientation of the UAV's camera by means of arrows whose colour change over time; (3) way-points: base position (blue circle), safety position (green circle), and person's position and orientation (pink circle and arrow).

Preprints (www.preprints.org) | NOT PEER-REVIEWED | Posted: 8 October 2020 doi:10.20944/preprints202010.0174.v1

Table 3. Values established in the simulation tests for each of the parameters under study; *relative monitoring altitude*, *monitoring velocity*, and *monitoring radius* (type/shape of trajectory).

Parameter	1st Value (Extreme 1)	2nd Value (Intermediate)	3rd Value (Extreme 2)
Relative Monitoring Altitude $z_r \Rightarrow z_m = z_p + z_r$	Low/Below $z_r = -0.30$ [m]	Medium/Centred $z_r = 0$ [m]	High/Above $z_r = +0.30m$ [m]
Monitoring Velocity $\omega_m = \omega_\gamma \cdot f_\omega$	Low Velocity $f_\omega = 0.65$	Medium Velocity $f_\omega = 1$	High Velocity $f_\omega = 1.35$
Monitoring Radius (Ellipse) R_x (Ellipse) R_y	Close to the Face $R_x = 0.90$ [m] $R_y = 1.70$ [m]	Equidistant (Circular) $R_x = 1.30$ [m] $R_y = 1.30$ [m]	Away from the Face $R_x = 1.70$ [m] $R_y = 0.90$ [m]

be noted that the information about the person is received from the VR Visualiser where the avatar is sitting on a couch (watching TV). In addition, the orientation of the UAV's camera is also represented by means of arrows whose colours change over time (the colour bar on the right side represents the time evolution during the complete simulation of 250 seconds). The results show how the trajectory planner is able to correctly generate the reference for the position and yaw angle of the UAV in each case. The accuracy of the GPI controller [22], which calculates the (control) inputs in order to reduce the tracking error of the trajectories to zero, is also checked. This ensures that the quadrotor model performs the monitoring flight accurately and according to the planner's references.

Table 4. Parameters defined in the UAV Simulator (MATLAB/Simulink® environment).

DESCRIPTION	VALUE	UNITS
Simulation		
Sample Time	$Ts = 0.01$	[s]
Simulation Time	$t = 250$	[s]
Quadrotor UAV		
Initial Position (Base Position)	$(x_b, y_b, z_b) = (0, 0, 0)$	[m]
Initial Yaw Angle	$\psi(0) = 0$	[rad]
Camera's Angle	$\alpha_{camera} = \pi/4$	[rad]
Mass	$m = 1$	[Kg]
Trajectory Planner		
Fixed Parameters:		
Velocity in Z axis [state 1 - landing/ state 11 - takeoff]	$v_z = [8.6 \cdot 10^{-2} / 4.3 \cdot 10^{-2}]$	[m/s]
Velocity in XY Diagonal Motion [state 3/ state 9]	$v_d = [0.1/0.2]$	[m/s]
Angular Velocity for Yaw Adjustment	$\omega_\psi = 3\pi/50$	[rad/s]
Angular Velocity for Ellipsoidal Motion	$\omega_\gamma = 9\pi/250$	[rad/s]
Timer of State 4 - Waiting in Safety Position	$t_{s4} = 5$	[s]
Timer of State 6 - Data Capture	$t_{s6} = 0$	[s]
Variable Parameters ⇒ see Table 3 and Figure 7		

4. Experimental Setup

The system described in this paper relies on the software and hardware platform described in [16]. It is a distributed architecture with two main modules: the UAV Simulator, in charge of reproducing the flight of the UAV considering its dynamics, and generating the trajectories; and the VR Visualiser, in charge of rendering the virtual UAV and its behaviour, as well as the virtual environment in which the UAV flight takes place. These two modules communicate with each other using the MQTT protocol, exchanging the position of the user, sent from VR Visualiser to UAV Simulator so that the trajectory based on the position of the user can be calculated, and the position of the UAV, sent from the UAV Simulator to the VR Visualiser to update the visual representation of the UAV. Figure 8 depicts this and shows the software tools used in the implementation of the architecture: MATLAB/Simulink®

Preprints (www.preprints.org) | NOT PEER-REVIEWED | Posted: 8 October 2020 doi:10.20944/preprints202010.0174.v1

for the UAV simulation, Unity3D to recreate the virtual home environment and Mosquitto as the open source MQTT broker selected.

As mentioned in Section 3, the UAV Simulator described in [16] has been extended to include the different options for the *relative monitoring altitude*, the *monitoring velocity* and the *monitoring radius*.

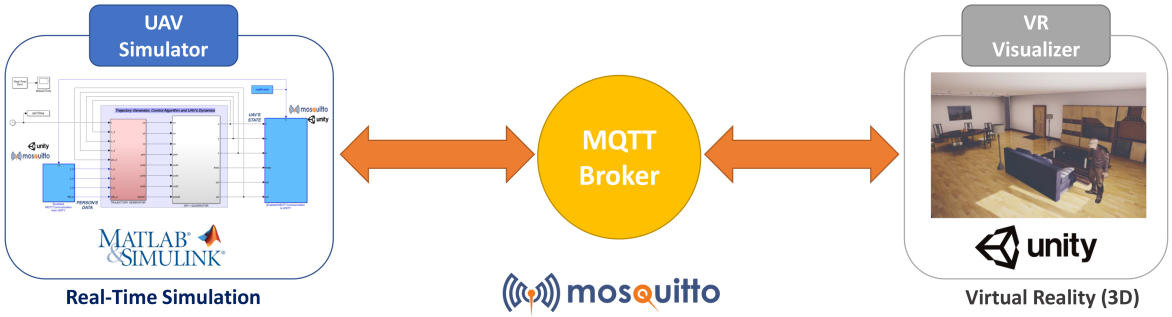

Figure 8. Architecture of the distributed platform.

4.1. Procedure

Unlike our previous work described in [16], and due to the restrictions imposed by the COVID-19 pandemic regarding the use of head mounted equipment covering the face of the users, three videos were created showcasing the different alternatives considered for *relative monitoring altitude, monitoring velocity* and *monitoring radius*. The participants received an email with a short description of the study and a link to an online questionnaire including the videos and some questions about it. The questionnaire was online from May 2020 to September 2020. It took an average time of 14 minutes to be filled by the participants in the evaluation.

4.2. Questionnaire

A questionnaire was designed using Microsoft Forms. It was divided into two main parts, a demographic questionnaire and a questionnaire about their preferences on the variables used in the study. This second questionnaire was designed specifically for this work, inspired by other approaches [24–26]. It was divided into three parts, one per each of the variables used in the study. For each part, a video was prepared showing each of the options per variable (i.e. three different flight heights) and then the participants had to answer to some questions regarding what they saw in the video and their preferences. There were a total amount of 36 questions, which were divided into preference questions, perceived safety, perceived supervision level, estimated distraction caused by the UAV flight and adequacy. A 5-point Likert scale ranging from strongly disagree to strongly agree was used to measure the responses.

4.3. Participants and Data Collection

Over 100 emails were sent to recruit participants and a total amount of 37 questionnaires were received. From them, 13 participants were female (35%) and 24 male (65%), while the total mean age was $M = 41.41$, $SD = 16.19$, $Max = 75$ and $Min = 22$. Regarding their use of technology, 70% of the participants stated they are advanced users, 25% are basic users and 5% prefer not to use technology in their daily lives.

4.4. Data Analysis

The data gathered through the questionnaires are described using descriptive statistics. They include measures of central tendency (mean and median) and dispersion (standard deviation, SD, and interquartile range, IQR) as well as percentages of responses in a given range of answers. The distribution of responses for the questionnaire is plotted as stacked horizontal histograms, and pie

Preprints (www.preprints.org) | NOT PEER-REVIEWED | Posted: 8 October 2020 doi:10.20944/preprints202010.0174.v1

charts are used to show the preference of the users about the different alternatives on *relative monitoring altitude, monitoring velocity* and *monitoring radius*. Since the data collected did not meet the requirements for normality (according to the Shapiro-Wilk test), the non-parametric Kruskal-Wallis test was used for null hypothesis testing in the comparison of different alternatives with a significance of 95%. In the cases in which the test found differences, the differences were studied using the Dunn's post-hoc test together and a Bonferroni correction for pair-wise comparisons. IBM SPSS Statistics (version 24) and Microsoft Excel were used to conduct the statistical analyses.

5. Results

The results are summarised in Table 5, as well as Figure 9 and Figure 10. Figure 10 uses pie charts to plot the preferences of the users regarding the variables under study. The preferred *relative monitoring altitude* is the highest one, which was selected by 78% of the participants (14% for low and 8% for medium). The difference in the preference for the *monitoring velocity* is not that big: 46% of the users selected high, 38% medium and 16% low. Finally, 54% of the participants selected the circular trajectory as their preferred one, followed by the elliptical trajectory when it is far from them (30%) and close to them (16%). Thus, the preferences are high altitude, high velocity and circular trajectory.

5.1. Results for Relative Monitoring Altitude

The results for the *safety*, *supervision*, and *distraction* questions are described in Table 5 and depicted in Figure 9. The results for *safety* show that users feel safer with the highest altitude, being the median value for this response 4 ($IQR = 1.00$) and having 81% of the responses in the rage 4-5 (positive answers: agree or strongly agree). This is in contrast with the medium (median value 2) and low (median value 3) altitudes. It is worth noting that the medium altitude had 51% of the responses in the range 1-2 (negative answers: disagree or strongly disagree). This result can be observed in Figure 9, being much more blue colour in A.Saf3. The Kruskal-Wallis test shows a significant difference in the results obtained for each different altitude ($\chi^2_{(2)} = 31.20$, $p < 0.001$), a post-hoc pairwise comparison revealed that this difference was between the highest altitude and the medium ($p<0.001$) and the lower ($p=0.001$), being the highest altitude perceived safer.

Regarding *supervision*, the median values obtained for the three different altitudes is 3, only differing in the IQR value: $IQR = 2$ for the highest altitude, and $IQR = 1$ for the medium and lower altitudes. A deeper look at the results show that medium and high altitudes had a similar percentage of positive answers (35% for high, 49% for medium and 24% for low) while all had similar percentage of negative answers (27%, 22% and 30%, respectively for high, medium and low). The Kruskal-Wallis test did not show any difference in the results for the three options ($\chi^2_{(2)} = 4.29$, $p = 0.117$).

Finally, for *distraction*, the median values were 2 ($IQR = 1$), 5 ($IQR = 1$) and 3 ($IQR = 2$) for high, medium and low altitudes respectively. The percentage of positive answers for each altitude (high, medium, low) were 19%, 89% and 68%, while the negative ones were 54%, 5% and 22%. This difference can be noticed with a quick look at the A.Dis section of Figure 9. The Kruskal-Wallis test found a difference in the values gathered for each altitude ($\chi^2_{(2)} = 41.92$, $p < 0.001$), being this difference between the high altitude and the other two ($p < 0.001$ for both), being the distraction lower for the high altitude.

5.2. Results for Monitoring Velocity

The median of the results for *safety* for the different *monitoring velocities* were 4 ($IQR = 2$), 4 ($IQR = 1$) and 4 ($IQR = 1$) for high, medium and low, respectively. The percentage of positive answers were 57%, 84% and 84%, while the percentage for negative answers were 27%, 3% and 5%. There was a significant difference in the data ($\chi^2_{(2)} = 9.97$, $p = 0.007$) and a post-hoc test showed that this difference was between high and low velocity ($p = 0.009$), stating that the users considered safer the lower velocity.

Preprints (www.preprints.org) | NOT PEER-REVIEWED | Posted: 8 October 2020 doi:10.20944/preprints202010.0174.v1

Table 5. Questionnaire and participants' responses.

Question	Mean	SD	Median	IQR
ALTITUDE				
Safety				
A.Saf1: I felt safe during the monitoring process by the UAV flying below my head	3.03	1.14	3.00	2.00
A.Saf2: I felt safe during the monitoring process by the UAV flying in front of my head	2.54	1.10	2.00	1.00
A.Saf3: I felt safe during the monitoring process by the UAV flying above my head	4.05	0.91	4.00	1.00
Supervision				
A.Sup1: I feel that there is too much supervision by the UAV flying below my head	2.89	1.02	3.00	1.00
A.Sup2: I feel that there is too much supervision by the UAV flying in front of my head	3.41	1.14	3.00	2.00
A.Sup3: I feel that there is too much supervision by the UAV flying above my head	3.05	1.03	3.00	1.00
Distraction				
A.Dis1: I think the UAV would distract me from my daily routine by flying below my head	3.76	1.26	4.00	2.00
A.Dis2: I think the UAV would distract me from my daily routine by flying in front of my head	4.35	0.82	5.00	1.00
A.Dis3: I think the UAV would distract me from my daily routine by flying above my head	2.43	1.04	2.00	1.00
VELOCITY				
Safety				
V.Saf1: I felt safe during the monitoring process by the UAV flying at a low velocity	4.19	0.84	4.00	1.00
V.Saf2: I felt safe during the monitoring process by the UAV flying at a medium velocity	4.11	0.74	4.00	1.00
V.Saf3: I felt safe during the monitoring process by the UAV flying at a high velocity	3.43	1.19	4.00	2.00
Supervision				
V.Sup1: I feel that there is too much supervision by the UAV flying at a low velocity	3.03	1.32	3.00	2.00
V.Sup2: I feel that there is too much supervision by the UAV flying at a medium velocity	3.49	0.87	4.00	1.00
V.Sup3: I feel that there is too much supervision by the UAV flying at a high velocity	3.30	1.15	3.00	2.00
Distraction				
V.Dis1: I think the UAV would distract me from my daily routine by flying at a low velocity	3.70	0.85	4.00	1.00
V.Dis2: I think the UAV would distract me from my daily routine by flying at a medium velocity	3.32	0.78	3.00	1.00
V.Dis3: I think the UAV would distract me from my daily routine by flying at a high velocity	2.97	0.80	3.00	0.00
Adequacy				
V.Ade1: I found the low velocity of the UAV adequate	3.54	1.37	4.00	3.00
V.Ade2: I found the medium velocity of the UAV adequate	3.22	1.16	3.00	1.00
V.Ade3: I found the high velocity of the UAV adequate	3.35	1.23	4.00	2.00
TRAJECTORY				
Safety				
T.Saf1: I felt safe during the monitoring process by the UAV flying elliptically (close to you)	2.70	1.10	2.00	2.00
T.Saf2: I felt safe during the monitoring process by the UAV flying following a circular trajectory	3.89	0.81	4.00	1.00
T.Saf3: I felt safe during the monitoring process by the UAV flying elliptically (far from you)	3.68	0.94	4.00	1.00
Supervision				
T.Sup1: I feel that there is too much supervision by the UAV flying elliptically (close to you)	2.68	1.20	2.00	2.00
T.Sup2: I feel that there is too much supervision by the UAV flying following a circular trajectory	3.84	0.69	4.00	1.00
T.Sup3: I feel that there is too much supervision by the UAV flying elliptically (far from you)	3.51	1.07	4.00	1.00
Distraction				
T.Dis1: I think the UAV would distract me from my daily routine by flying elliptically (close to you)	3.51	1.07	3.00	1.00
T.Dis2: I think the UAV would distract me from my daily routine by flying following a circular trajectory	2.89	0.70	3.00	1.00
T.Dis3: I think the UAV would distract me from my daily routine by flying elliptically (far from you)	2.89	0.81	3.00	1.00
Adequacy				
T.Ade1: I found the UAV's monitoring distance to be correct by the UAV flying elliptically (close to you)	3.86	1.03	4.00	1.00
T.Ade2: I found the UAV's monitoring distance to be correct by the UAV flying following a circular trajectory	2.84	0.99	3.00	2.00
T.Ade3: I found the UAV's monitoring distance to be correct by the UAV flying elliptically (far from you)	2.95	1.05	3.00	2.00

The medians for the *supervision* data gathered for high, medium and low velocity were 3 ($IQR = 2$), 4 ($IQR = 1$) and 3 ($IQR = 2$), respectively. The percentages of positive answers were 49%, 54% and 43%. The percentages of negative answers were 32%, 11% and 38%. Despite the differences in the data (also apparent in Figure 9), the Kruskal-Wallis test could not find statistically significant differences between them ($\chi^2_{(2)} = 2.25$, p = 0.324).

Regarding *distraction*, the median values were 3 ($IQR = 0$) for high velocity, 3 ($IQR = 1$) for medium velocity and 4 ($IQR = 1$) for low velocity. The percentage for positive answers was 16%, 35% and 57% and the percentage of negative answers was 22%, 11% and 5%, respectively. In this case, the data look similar in Figure 9, but the Kruskal-Wallis test found a statistically significant difference between them ($\chi^2_{(2)} = 14.06$, p = 0.001), and the post-hoc test found that the difference was between the low and high velocities (p = 0.001), being the level of perceived distraction higher for the low velocity.

The median values obtained for the *adequacy* questions for velocity were 4 ($IQR = 2$) for high, 3 ($IQR = 1$) for medium and 4 ($IQR = 3$) for low velocity. The percentage of positive answers were 51%,

Preprints (www.preprints.org) | NOT PEER-REVIEWED | Posted: 8 October 2020 doi:10.20944/preprints202010.0174.v1

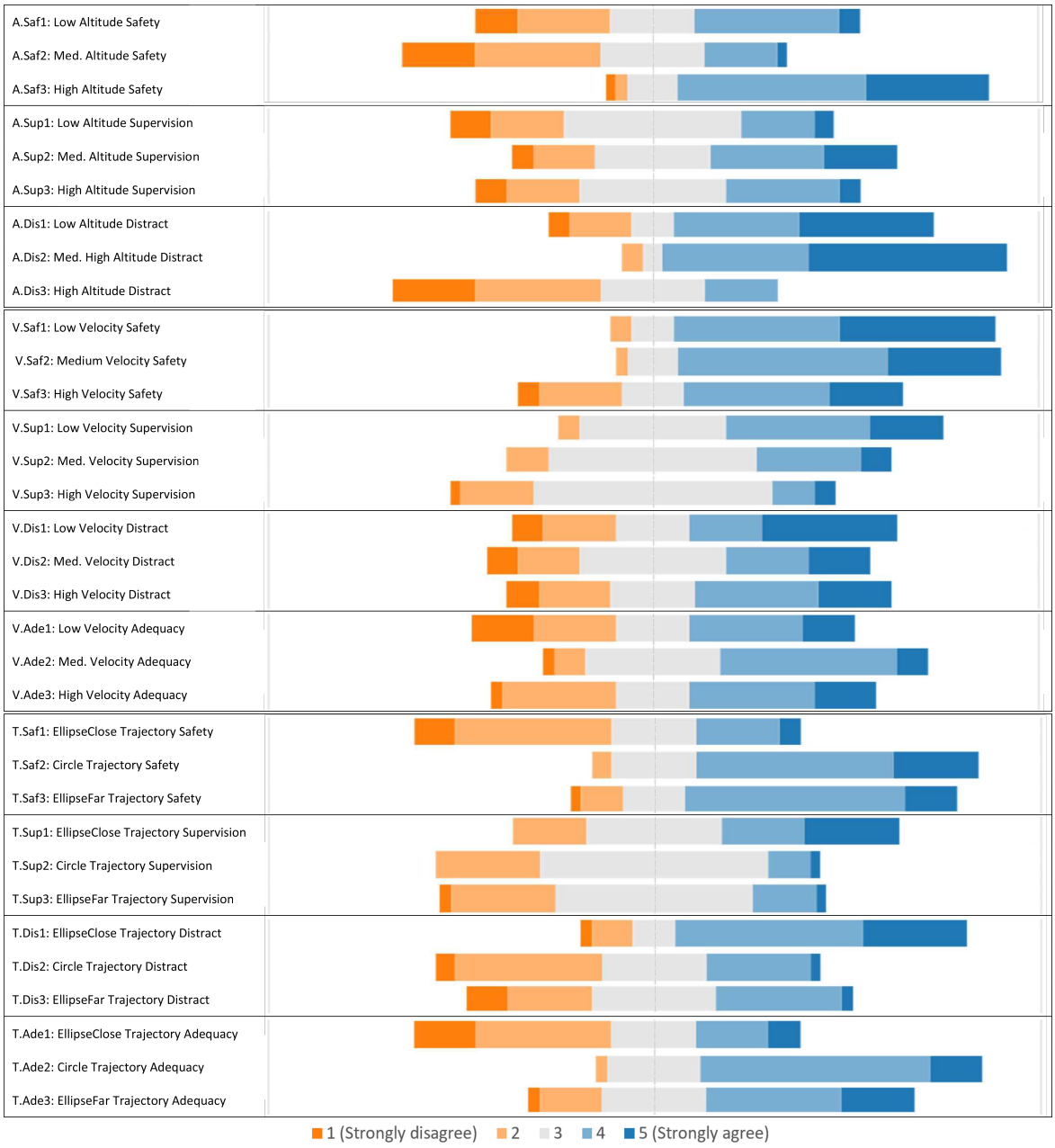

Figure 9. Distribution of responses for each question.

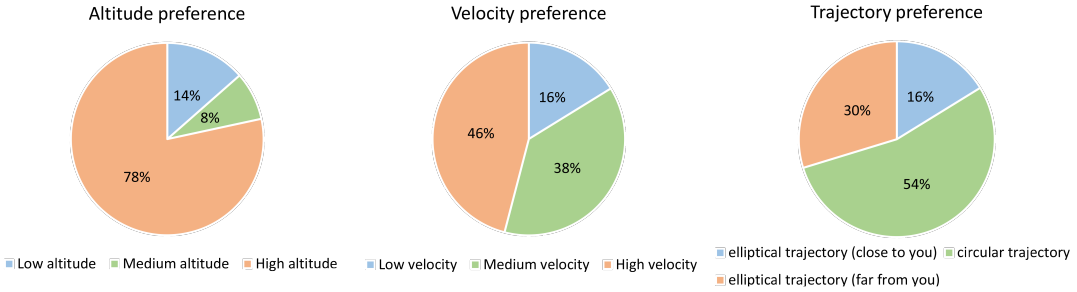

Figure 10. User preference for each of the variables measured.

38% and 54%, while the negative ones were 27%, 24% and 27%, respectively. This time, there were no statistically significant differences between the responses of the three groups ($\chi^2_{(2)}$ = 1.50, p = 0.473).

Preprints (www.preprints.org) | NOT PEER-REVIEWED | Posted: 8 October 2020 doi:10.20944/preprints202010.0174.v1

5.3. Results for Monitoring Radius

The last group of questions was about the *monitoring radius* followed by the UAV during the monitoring process. The median values obtained for *safety* were 4 ($IQR = 1$) for the elliptical trajectory far from the user, 4 ($IQR = 1$) for the circular trajectory and 2 ($IQR = 2$) for the elliptical trajectory close to the user. The percentage of positive answers were 70%, 73% and 27%, while it was 14%, 5% and 51% for the negative answers, respectively. The difference is noticeable this time with a quick look at the T.Saf block in Figure 9, and it was confirmed by the Kruskal-Wallis test ($\chi^2_{(2)} = 23.86$, $p < 0.001$). The post-hoc test revealed that the difference was between the elliptical trajectory close to the user and both the circular ($p < 0.001$) and the elliptical trajectory far from the user ($p < 0.001$), being the perceived safety lower for the trajectory close to the user.

The medians for *supervision* were 4 ($IQR = 1$) for the elliptical trajectory far from the user, 4 ($IQR = 1$) for the circular trajectory and 2 ($IQR = 2$) for the elliptical trajectory close to the user. The percentage of positive answers were 54%, 73% and 27%, while it was 19%, 3% and 51% for the negative answers, respectively. There was a significant difference ($\chi^2_{(2)} = 19.65$, $p < 0.001$) between the elliptical trajectory close to the user and the circular trajectory ($p < 0.001$) and the elliptical trajectory far from the user ($p = 0.007$). The post-hoc test states that the perceived level of supervision is higher for the trajectory close to the user.

About *distraction*, the median values for *monitoring radius* were 3 ($IQR = 1$) for the elliptical trajectory far from the user, 3 ($IQR = 1$) for the circular trajectory and 3 ($IQR = 1$) for the elliptical trajectory close to the user. The percentage of positive answers were 19%, 14% and 46%, while it was 30%, 27% and 19% for the negative answers, respectively. There was a significant difference in the responses ($\chi^2_{(2)} = 8.78$, $p < 0.012$), being the level of distraction higher for the trajectory close to the user as compared to the circular trajectory ($p = 0.028$) and the elliptical trajectory far from the user ($p = 0.034$).

Finally, the median values regarding *adequacy* were 3 ($IQR = 2$), 3 ($IQR = 2$) and 4 ($IQR = 1$). The percentage of positive answers were 35%, 30% and 76%, while it was 32%, 43% and 14% for the negative answers, respectively. The Kruskal-Wallis test found a difference in the values gathered for each *monitoring radius* ($\chi^2_{(2)} = 20.15$, $p < 0.001$), being this difference between the elliptical trajectory close to the user and the other two ($p = 0.001$ for the circular trajectory and $p < 0.001$ for elliptical trajectory far from the user), being the adequacy lower for the trajectory close to the user.

6. Discussion

This paper belongs to a research line in socially assistive UAVs with potential for dependent people, including ageing adults. The paper has presented an assistive UAV whose mission is to perform a monitoring flight from time to time to determine a person's condition and a possible assistance. This monitoring flight basically consists of a series of manoeuvres to take-off, get close to the person, fly around the person to obtain facial images and then return to its base. Moreover, a survey was conducted to evaluate the users' sense of safety and comfort in a VR home environment.

The 37 participants evaluated different parameters of the UAV's trajectory during the monitoring process. The main aim of this evaluation was to study the impact of different alternatives for three key parameters of the monitoring process of an assistive UAV: the *relative monitoring altitude*, the *monitoring velocity* and the *monitoring radius*. For each parameter, three alternatives were implemented in our simulation platform and tested using a VR environment. The user preferences were consistent with the answers they provided about questions regarding the perceived *safety*, *supervision*, *distraction* and *adequacy*.

High altitude was selected as the more appropriate altitude for the UAV monitoring process by most users. At the same time, it was perceived as the safer one, followed by the lower altitude. It may be possible because the users felt that it may avoid collisions with the UAV, which could be dangerous specially at the user head level (medium altitude). Regarding the perceived supervision level, no significant differences could be found, despite being the medium altitude perceived slightly more

 doi:10.20944/preprints202010.0174.v1

negative than the other two. For distraction, the highest altitude was perceived to cause the lower level of distraction in a statistically significant manner, probably because it was far from their line of sight. Therefore, it seems reasonable to think that the highest altitude is the best one for monitoring processes.

High velocity was considered as the more appropriate one for monitoring, closely followed by medium velocity. However, it was perceived as less safe than the low velocity, although no difference could be found in the perceived level of supervision. That was not the case for distraction, were 57% of the responses agreed or strongly agreed that the UAV would distract them flying at low velocity. There was a statistically significant difference with the high velocity, at it may be due to the fact that the UAV flying at low velocity stays a larger period of time flying around the user, increasing the chances for distraction. Regarding the adequacy of the monitoring velocities, the data gathered was very similar for all of them, so no statistically significant difference could be found. In this case, either the high or the medium velocity could be selected when designing the monitoring process of a UAV, the highest one is preferred by the users, but at the same time they felt less safe with it.

The circular trajectory was selected by most of the users as their preferred one, while the elliptical trajectory passing close to them was the one they liked the least. This is confirmed with the results for safety, supervision and distraction, as it is perceived as less safe, with too much supervision and causing more distractions to them. There are no statistically significant difference between circular and elliptical trajectory passing far from the user, only a slightly higher perceived supervision for the circular one, which could be related to the fact that the trajectory passes closer to the user. Thus, according to the data gathered, the circular trajectory would be preferred over elliptical ones, but the elliptical trajectory passing far from the user could be also a good choice according to safety, supervision level and distraction.

The limitations of this evaluation are related to the difficulties of performing face-to-face experiments using VR facilities. Due to the current situation derived from the COVID-19 pandemic, a series of videos were shown to the participants. The validation through videos, and not in an immersive VR environment, may have distorted some of the results. The authors, therefore, will hopefully repeat the experiments in a close future. In addition, the sample size must also be incremented to reinforce the current conclusions derived from the study.

Nonetheless, the authors believe that using VR as an alternative to physical prototyping saves time, provides a high flexibility and enables iterative testing possibilities in the design of socially assistive technologies incorporating different aspects of user trust in automation.

Author Contributions: L.M.B., A.S.G., R.M., J.L.V. and A.F.-C. conceived, designed and evaluated the proposed trajectory planning algorithm and managed the study with participants. Additionally, L.M.B., A.S.G., R.M., J.L.V. and A.F.-C. analysed the data and participated in writing the paper.

Funding: The work leading to this paper has received funding from the iRel4.0 project (H2020-ECSEL grant agreement no 876659; Spain's Agencia Estatal de Investigación grant no PCI2020-112240), VALU3S project (H2020-ECSEL grant agreement no 876852; Spain's Agencia Estatal de Investigación grant no PCI2020-112001), MICINN Scientific and Technical Equipment (grant no EQC2019-006063-P), Treasure (JCCM grant no SBPLY/19/180501/000270; EC's European Regional Development Fund) projects, Ramon y Cajal Program (Spain's MICINN grant no RYC-2017-22836; EC's European Social Fund), and CIBERSAM (Biomedical Research Networking Center in Mental Health).

Conflicts of Interest: The authors declare no conflict of interest.

Abbreviations

The following abbreviations are used in this manuscript:

GPI	Generalised Proportional Integral
HRI	Human-Robot Interaction
MQTT	Message Queue Telemetry Transport
UAV	Unmanned Aerial Vehicle
VR	Virtual Reality
SD	Standard Deviation
IQR	Interquartile Range

References

1. Nocentini, O.; Fiorini, L.; Acerbi, G.; Sorrentino, A.; Mancioppi, G.; Cavallo, F. A Survey of Behavioral Models for Social Robots. *Robotics* **2019**, *8*, 54. doi:10.3390/robotics8030054.
2. Wojciechowska, A.; Frey, J.; Mandelblum, E.; Amichai-Hamburger, Y.; Cauchard, J.R. Designing Drones: Factors and Characteristics Influencing the Perception of Flying Robots. In *Proceedings of the ACM on Interactive, Mobile, Wearable and Ubiquitous Technologies*; Association for Computing Machinery: New York, NY, USA, 2019; Vol. 3, p. 111. doi:10.1145/3351269.
3. Martín Rico, F.; Rodríguez-Lera, F.; Clavero, J.; Guerrero-Higueras, A.; Matellán Olivera, V. An Acceptance Test for Assistive Robots. *Sensors* **2020**, *20*, 3912. doi:10.3390/s20143912.
4. Cavallo, F.; Esposito, R.; Limosani, R.; Manzi, A.; Bevilacqua, R.; Felici, E.; Di Nuovo, A.; Cangelosi, A.; Lattanzio, F.; Dario, P. Robotic Services Acceptance in Smart Environments With Older Adults: User Satisfaction and Acceptability Study. *Journal of Medical Internet Research* **2018**, *20*, e264. doi:10.2196/jmir.9460.
5. Garcia-Salguero, M.; Gonzalez-Jimenez, J.; Moreno, F.A. Human 3D Pose Estimation with a Tilting Camera for Social Mobile Robot Interaction. *Sensors* **2019**, *19*, 4943. doi:10.3390/s19244943.
6. Lewis, M.; Sycara, K.; Walker, P. The Role of Trust in Human-Robot Interaction. In *Foundations of Trusted Autonomy*; Springer, Cham, 2018; pp. 135–159.
7. McMurray, J.; Strudwick, G.; Forchuk, C.; Morse, A.; Lachance, J.; Baskaran, A.; Allison, L.; Booth, R. The Importance of Trust in the Adoption and Use of Intelligent Assistive Technology by Older Adults to Support Aging in Place: Scoping Review Protocol. *JMIR Research Protocols* **2017**, *6*, e218. doi:10.2196/resprot.8772.
8. Yusif, S.; Soar, J.; Hafeez-Baig, A. Older people, assistive technologies, and the barriers to adoption: A systematic review. *International Journal of Medical Informatics* **2016**, *94*, 112–116. doi:10.1016/j.ijmedinf.2016.07.004.
9. Okamura, K.; Yamada, S. Adaptive trust calibration for human-AI collaboration. *PLOS ONE* **2020**, *15*, 1–20. doi:10.1371/journal.pone.0229132.
10. Hoffman, R.R.; Johnson, M.; Bradshaw, J.M.; Underbrink, A. Trust in Automation. *IEEE Intelligent Systems* **2013**, *28*, 84—88. doi:10.1109/MIS.2013.24.
11. Langer, A.; Feingold-Polak, R.; Mueller, O.; Kellmeyer, P.; Levy-Tzedek, S. Trust in socially assistive robots: Considerations for use in rehabilitation. *Neuroscience & Biobehavioral Reviews* **2019**, *104*, 231–239. doi:10.1016/j.neubiorev.2019.07.014.
12. Song, Y.; Luximon, Y. Trust in AI Agent: A Systematic Review of Facial Anthropomorphic Trustworthiness for Social Robot Design. *Sensors* **2020**, *20*, 5087. doi:10.3390/s20185087.
13. Gompei, T.; Umemuro, H. Factors and Development of Cognitive and Affective Trust on Social Robots. Social Robotics; Ge, S.S.; Cabibihan, J.J.; Salichs, M.A.; Broadbent, E.; He, H.; Wagner, A.R.; Castro-González, Á., Eds.; Springer International Publishing: Cham, 2018; pp. 45–54.
14. de Graaf, M.M.; Allouch, S.B.; Klamer, T. Sharing a life with Harvey: Exploring the acceptance of and relationship-building with a social robot. *Computers in Human Behavior* **2015**, *43*, 1–14. doi:10.1016/j.chb.2014.10.030.
15. Mcknight, D.H.; Carter, M.; Thatcher, J.B.; Clay, P.F. Trust in a Specific Technology: An Investigation of Its Components and Measures. *ACM Transactions on Management Information Systems* **2011**, *2*, 12. doi:10.1145/1985347.1985353.
16. Belmonte, L.; Garcia, A.S.; Segura, E.; Novais, P.J.; Morales, R.; Fernandez-Caballero, A. Virtual Reality Simulation of a Quadrotor to Monitor Dependent People at Home. *IEEE Transactions on Emerging Topics in Computing* **2020**. doi:10.1109/TETC.2020.3000352.

17. Sadka, O.; Giron, J.; Friedman, D.A.; Zuckerman, O.; Erel, H. Virtual-reality as a Simulation Tool for Non-humanoid Social Robots. In *Extended Abstracts of the 2020 CHI Conference on Human Factors in Computing Systems*; Association for Computing Machinery: New York, NY, USA, 2020; pp. 1–9. doi:10.1145/3334480.3382893.
18. Templin, T.; Popielarczyk, D. The Use of Low-Cost Unmanned Aerial Vehicles in the Process of Building Models for Cultural Tourism, 3D Web and Augmented/Mixed Reality Applications. *Sensors* **2020**, *20*, 5457. doi:10.3390/s20195457.
19. Górriz, J.M.; Ramírez, J.; Ortíz, A.; Martínez-Murcia, F.J.; Segovia, F.; Suckling, J.; Leming, M.; Zhang, Y.D.; Álvarez-Sánchez, J.R.; Bologna, G.; others. Artificial intelligence within the interplay between natural and artificial computation: Advances in data science, trends and applications. *Neurocomputing* **2020**, *410*, 237–270. doi:10.1016/j.neucom.2020.05.078.
20. Martinez-Gomez, J.; Fernández-Caballero, A.; Garcia-Varea, I.; Rodriguez, L.; Romero-Gonzalez, C. A taxonomy of vision systems for ground mobile robots. *International Journal of Advanced Robotic Systems* **2014**, *11*, 111. doi:10.5772/58900.
21. Marín-Morales, J.; Llinares, C.; Guixeres, J.; Alcañiz, M. Emotion Recognition in Immersive Virtual Reality: From Statistics to Affective Computing. *Sensors* **2020**, *20*, 5163. doi:10.3390/s20185163.
22. Fernández-Caballero, A.; Belmonte, L.M.; Morales, R.; Somolinos, J.A. Generalized proportional integral control for an unmanned quadrotor system. *International Journal of Advanced Robotic Systems* **2015**, *12*, 85. doi:10.5772/60833.
23. Belmonte, L.M.; Morales, R.; García, A.S.; Segura, E.; Novais, P.; Fernández-Caballero, A. Trajectory Planning of a Quadrotor to Monitor Dependent People. In *Understanding the Brain Function and Emotions*; Springer International Publishing, 2019; pp. 212–221. doi:10.1007/978-3-030-19591-5_22.
24. Dockx, K.; Alcock, L.; Bekkers, E.; Ginis, P.; Reelick, M.; Pelosin, E.; Lagravinese, G.; Hausdorff, J.M.; Mirelman, A.; Rochester, L.; others. Fall-prone older people's attitudes towards the use of virtual reality technology for fall prevention. *Gerontology* **2017**, *63*, 590–598.
25. Ninomiya, T.; Fujita, A.; Suzuki, D.; Umemuro, H. Development of the Multi-dimensional Robot Attitude Scale: Constructs of people's attitudes towards domestic robots. International Conference on Social Robotics. Springer, 2015, pp. 482–491.
26. Chiari, L.; van Lummel, R.; Pfeiffer, K.; Lindemann, U.; Zijlstra, W. Deliverable 2.2: Classification of the user's needs, characteristics and scenarios-update. *Unpublished report from the EU Project (6th Framework Program, IST Contract no. 045622) Sensing and Action to support mobility in Ambient Assisted Living]. Department of Health* **2009**.